

Electrical Control of Exciton-Polariton Condensate Josephson Junctions

Hua Wang,^{*} Hong-Yi Xie,[†] and Kieran Mullen

*Homer L. Dodge Department of Physics and Astronomy, Center for Quantum Research and Technology,
The University of Oklahoma, Norman, Oklahoma 73069, USA*

(Dated: March 5, 2024)

We propose the electrical control of a device probing the Josephson effect in exciton-polariton (EP) condensates, which can be switched between various dynamical modes. We model the device by a four-component Gross-Pitaevskii equation assuming that ideal EP condensates are established with well-balanced pumping and dissipation. All the model parameters are calculated microscopically. In particular, we obtain the polariton tunneling strength across the junction as a second-order process of electron-hole pair tunneling. We find that the EP condensates can be manipulated through distinctive degrees of freedom not present in other coherent quantum systems, and the dynamics of EP Josephson junctions are far richer than that of the conventional superconducting junctions.

Quantum coherence has been observed in a host of many-body systems in a broad range of temperatures, from Bose-Einstein condensates of alkali metal vapors at nanokelvins [1, 2] to exotic states in cuprates [3] that persist up to ~ 130 K [4]. Intensive studies of these systems have enriched our understanding of the fascinating physics of quantum coherence and correlations [5], and stimulated the development of technologies built upon the quantum-coherent nature, such as quantum computation [6], quantum communication [7], quantum sensing [8], and quantum simulation [9].

One less-explored system is the exciton-polariton (EP) condensate [10–12], a quantum fluid of hybrid bosons that are coherent superpositions of cavity photons and excitons – composite bosons consisting of electrons and holes bound by Coulomb interactions [13]. Upper-polariton (UP) and lower-polariton (LP) branches are formed due to exciton-photon hybridization [Fig. 1(a)]. Excitons created by the laser pump relax into the EP condensate around the LP band bottom, and a steady state can be established when the spontaneously decaying population are compensated. The cavity polaritons are regarded as potential candidates for realizing the room-temperature superfluidity [14–20], because their effective masses are extremely low [10]. Due to charge neutrality, the EP condensates are less susceptible to interactions that can cause the loss of condensate-phase coherence, even though the lifetime of an individual polariton is as short as picoseconds, which is limited by cavity photon leaking [11]. Moreover, compared to pure excitons, the cavity polaritons are less sensitive to the potential variations in solids, and the EP condensate phase coherence can be detected in higher-order optical coherence measurements, attributed to their photon components [21, 22].

To date, the EP condensates are usually created, manipulated, and monitored through optical approaches in most experiments [10, 14–20]. Nevertheless, the optical

cavity is also intrinsically compatible with the powerful tools of nanofabrication, by which an electric interface can be created and the local dynamics of an EP condensate can be electrically driven and detected on a short time scale. In this letter, we propose a Josephson junction formed by two EP-condensates, which can be electrically switched between various dynamical modes, as sketched in Fig. 1(b). We find that the EP condensates can be manipulated through distinctive degrees of freedom not present in other coherent quantum systems, and the dynamics of EP Josephson junctions are far richer than that of the conventional superconducting junctions.

Four-component Gross-Pitaevskii equation. As shown in Fig. 1(b), we consider two semiconductor thin layers horizontally separated by a tunneling barrier. Each layer is encapsulated between two conductor plates and an in-plane electric field can be generated and controlled by an external voltage source. The semiconductor device is embedded in an optical microcavity and we assume only one longitudinal cavity mode within the semiconductor band gap, which can hybridize with the subgap excitons. The transverse momentum is not constrained and the resulting dispersion is parabolic along \mathbf{k}_{\parallel} with a small effective mass $\sim 10^{-5}m_e$ [11], where m_e is the mass of a free electron. As shown in Fig. 1(a), near $\mathbf{k}_{\parallel} = 0$, where the photon mode is in resonance with the exciton mode, both lower and upper polaritons are equal-weighted superpositions of a photon and an exciton. The EP condensation of either branch occurs when the states in the vicinity of $k_{\parallel} = 0$ are macroscopically occupied. In practice, a blue-detuned cavity is often used to optimize the thermalization time when the experiment only focuses on the LP branch. The time scales for the condensate formation and decay will be discussed at the end of the paper.

We assume that the semiconducting flakes are sufficiently small so that the spatial variations of the condensate density within either region can be neglected. The dynamics of the UP and LP condensates confined on the left and right side of the device can then be described by the four-component Gross-Pitaevskii equation (GPE). We introduce the complex variables ψ_{κ} and χ_{κ} to describe the macroscopic amplitude of the polariton

^{*} hua.wang.phys@ou.edu

[†] hongyi.xie-1@ou.edu

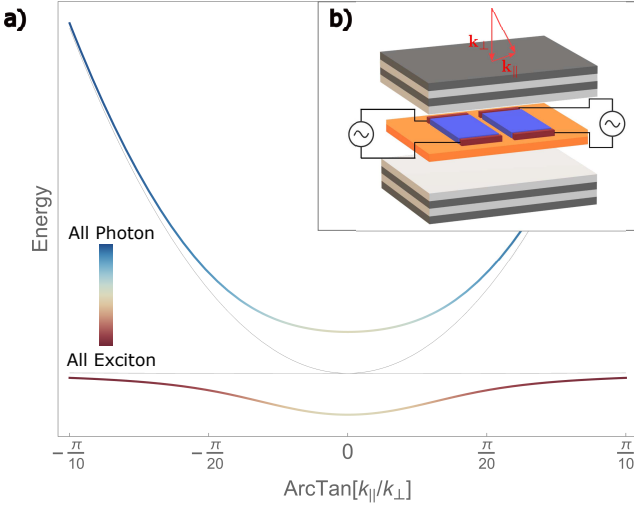


FIG. 1. Schematics of cavity polaritons and EP Josephson junctions. (a) Typical energy dispersions of cavity polariton along in-plane momentum of incident light k_{\parallel} . Upper and lower polariton branches are formed due to strong exciton-photon hybridization at $k_{\parallel} = 0$. The color codes of the lower (upper) branch represent the weight of exciton(photon). (b) Schematic geometry of an EP junction. The two-dimensional device is defined via nanofabrication of a semiconducting material such as GaAs, embedded in an optical cavity formed by distributed Bragg reflectors and continuously pumped by an incident laser. Two adjacent plates attached to the semiconductor allow the application of an in-plane electric field, which polarizes the EP condensate as well as provides a measure of the local capacitance.

ground state $\phi_{\kappa}(\mathbf{r})$ for the LP and UP condensates, respectively, where $\kappa \in \{L, R\}$ denotes the left (L) and right (R) side of the junction. The time evolution of the lower polariton condensates is described by

$$\begin{aligned}
 i\hbar \frac{\partial \psi_L}{\partial t} &= \left(-\frac{\mu_{LR} + \mu_{UL}}{2} + \frac{U}{4} |\psi_L|^2 + \frac{U}{2} |\chi_L|^2 \right) \psi_L \\
 &+ U \left(\frac{1}{4} \psi_L^* \chi_L + \frac{1}{2} \left(|\psi_L|^2 + |\chi_L|^2 \right) \right) \chi_L \\
 &- J (\psi_R + \chi_R), \\
 i\hbar \frac{\partial \psi_R}{\partial t} &= \left(\frac{\mu_{LR} - \mu_{UL}}{2} + \frac{U}{4} |\psi_R|^2 + \frac{U}{2} |\chi_R|^2 \right) \psi_R \\
 &+ U \left(\frac{1}{4} \psi_R^* \chi_R + \frac{1}{2} \left(|\psi_R|^2 + |\chi_R|^2 \right) \right) \chi_R \\
 &- J (\psi_L + \chi_L), \tag{1}
 \end{aligned}$$

where μ_{LR} is the energy difference between the left and right LP condensates, μ_{UL} is the energy difference between LP and UP condensates on one side, U is the interaction energy arising from the scattering of the exciton components of polaritons, and J is the tunneling energy for the exciton component to go between the left and

right side. Two similar equations describe the upper EP condensate, obtained by exchanging $\psi \leftrightarrow \chi$ and replacing $\mu_{UL} \rightarrow -\mu_{UL}$. We discuss the assumptions behind, and values of these parameters below.

The energy difference μ_{UL} is determined by the vacuum Rabi splitting at $k_{\parallel} = 0$. The left-right bias potential μ_{LR} is controlled by the in-plane electric fields applied to the two semiconductors. The exciton components are polarizable, and the polarizability α can be estimated by perturbation theory in terms of exciton orbital wavefunctions, which resembles that of a 2D hydrogen atom [23]

$$\alpha = -e^2 \sum_{n,l=\pm 1} \frac{|\langle \Phi_{10} | \hat{\mathbf{x}} | \Phi_{nl} \rangle|^2}{E_{10} - E_{nl}}$$

where Φ_{nl} is the 2D electron-hole orbital wavefunction in principle quantum number n and angular quantum number l , and E_{nl} the corresponding eigen-energy, $\hat{\mathbf{x}}$ is the e-h displacement operator in the direction of the applied electric field $\mathcal{E}_{L/R}$. In consequence, $\mu_{LR} = \alpha (\mathcal{E}_L^2 - \mathcal{E}_R^2) / 2$. For excitons in GaAs [24], we estimate $\alpha \sim 10^{-3} e^2 \mu\text{m}^2 \text{eV}^{-1}$. A sample-homogeneity-induced energy difference can be zeroed out by tuning the applied electric fields. We note that an out-of-plane electric field can strongly modify the inter-polariton interaction strength [25], and, therefore, it should be prohibited for the application of the device.

We assume that the left and right excitons couple to the same cavity modes and the polariton tunneling energy J is purely determined by exciton tunneling processes through the inverse Hopfield transformation [11]. Up to second order in single-electron/hole tunneling strength, we obtain

$$\begin{aligned}
 J &= t_e t_h \sum_{\mathbf{k}} \Phi_{\nu', \mathbf{K}}^*(\mathbf{k}) \Phi_{\nu, \mathbf{K}}(\mathbf{k}) \\
 &\times \left(\frac{1}{E_{\nu \mathbf{K}} - \epsilon_{\mathbf{k}, \mathbf{K}-\mathbf{k}}} + \frac{1}{E_{\nu' \mathbf{K}} - \epsilon_{\mathbf{k}, \mathbf{K}-\mathbf{k}}} \right). \tag{2}
 \end{aligned}$$

Here $\Phi_{\nu, \mathbf{K}}(\mathbf{k})$ is the Fourier component of the wavefunction of the 2D exciton in ν -orbital, with \mathbf{K} being the center-of-mass (COM) momentum, $E_{\nu \mathbf{K}}$ is the exciton-band energy, $\epsilon_{\mathbf{k}, \mathbf{k}'}$ is the energy of an electron at momentum \mathbf{k} and hole at momentum \mathbf{k}' in the absence of interactions, and $t_{e,h}$ are the single-particle tunneling energy for the electrons and holes, which are material- and device-geometry dependent can be related to the conductance of the semiconductor device in the absence of cavity. The derivation of Eq. (2) can be found in Supplemental Material. For 2D excitons in 1s state, we evaluate $J = -(16\pi^2/3)(t_e t_h) / (|E_0|)$, where $|E_0| = \hbar^2 / (2\mu a^2)$ is the binding energy, with a being the Bohr radius and μ the reduced mass of an electron-hole pair. We note that our EP junction device is different from the one studied in Ref. 26, where the Josephson energy is determined by the tunneling processes of cavity photons. In principle,

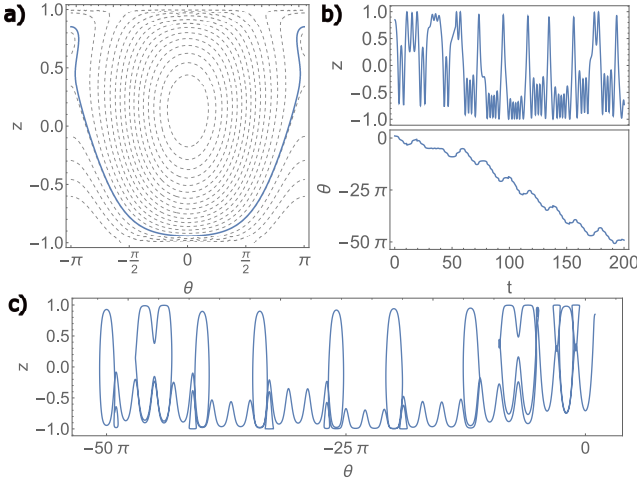


FIG. 2. Stable and chaotic dynamics in LP-only Josephson junctions [Eq. (3)]. We take $\Lambda = 2$ and $z_0 = 0.2$. (a) Energy contour in phase space for static driving potential $z_1 = 0$. For the initial conditions $z(0) = 0.85$ and $\theta(0) = \pi$, the system follows the blue trajectory. (b) Time evolution of density (upper panel) and phase (lower panel) for dynamical driving potential $z_1 = 0.4$. The phase-space trajectory exhibits chaotic behavior as shown in (c).

the Josephson energy in our device is highly tunable by varying the barrier potential between two semiconductors.

The interaction energy U arises from the s-wave scattering of the excitons, which can be estimated as $U = g_s \int |\phi(\mathbf{r})|^4 d^2\mathbf{r}$, for simplicity we assume symmetric macroscopic wavefunctions $\phi_L(\mathbf{r}) = \phi_R(\mathbf{r}) = \phi(\mathbf{r})$ and g_s is the scattering magnitude. Expressing an exciton as the superposition of an LP and an UP, we obtain the EP interactions in Eq. (1). The magnitude of g_s is usually characterized by the blue shift of LP dispersion [27]. In a GaAs-based 2D layer with unspecified geometry we estimate g_s of the order of $1 \sim 10 \mu\text{eV}\mu\text{m}^2$. Since the Josephson energy J is highly tunable, one could study the interplay between the Josephson effect and the non-linearity induced by interactions.

Results. We consider two major cases. In the first, the coherent excitation in the upper polariton branch is negligible, and the coupled equations reduce to the two-component bosonic junction model that has been intensively studied [28]. Defining the dimensionless interaction strength $\Lambda = UN_T/2J$ and time $\tau = \frac{2J}{\hbar}t$ in LP parameters, where $N_T = |\psi_L|^2 + |\psi_R|^2$, and parametrizing $\psi_{L,R} = \sqrt{N_T(1 \pm z)}/2 e^{i\theta_{L,R}}$ with $|z| \leq 1$, we transform Eq. (1) to

$$\dot{\theta} = \Lambda(z - z_b(\tau)) + \frac{z \cos \theta}{\sqrt{1 - z^2}}, \quad \dot{z} = -\sqrt{1 - z^2} \sin \theta, \quad (3)$$

where $\theta = \theta_R - \theta_L$. We note that the conjugate variables $\{z, \theta\}$ form the phase space of the dynamical system.

For time-independent bias potential $z_b(\tau) = \text{Const.}$, such a system resembles the undriven non-linear pendu-

lum. Its dynamics fall into two categories: those where the trajectory is a closed loop in phase space; and those in which a pendulum would swing through the complete circle, so the trajectory is unbounded. The latter are termed “macroscopic quantum self-trapping” modes [28], meaning the condensate density difference remains non-zero. Both types of modes are present in the energy contours [Fig. 2(a)]. When the bias potential has a constant and an oscillating component $z_b(\tau) = z_0 + z_1 \sin(\Omega\tau)$, it is possible to switch between different trajectories within the same dynamical category. However, the modes near the separatrix are unstable, and the dynamical potential can lead to chaotic behavior [Fig. 2(b)].

The second major case is that both the LP and UP condensates are non-negligible so that the system must be described by the four-component model. Switching to the dimensionless variables $g = U/J$, $\delta = \mu_{LR}/J$, and $\Delta = \mu_{UL}/J$, and performing a rotating-frame transformation (see Supplemental Material), we rewrite Eq. (1) in the matrix form

$$i\partial_\tau \begin{pmatrix} \tilde{\psi}_L \\ \tilde{\psi}_R \\ \tilde{\chi}_L \\ \tilde{\chi}_R \end{pmatrix} = \begin{pmatrix} h_{LP} & v \\ v^\dagger & h_{UP} \end{pmatrix} \begin{pmatrix} \tilde{\psi}_L \\ \tilde{\psi}_R \\ \tilde{\chi}_L \\ \tilde{\chi}_R \end{pmatrix} \quad (4)$$

where the blocks of the effective Hamiltonian read

$$h_{LP} = \begin{pmatrix} \frac{\delta}{2} + \frac{g}{4}|\tilde{\psi}_L|^2 + \frac{g}{2}|\tilde{\chi}_L|^2 & -1 \\ -1 & -\frac{\delta}{2} + \frac{g}{4}|\tilde{\psi}_R|^2 + \frac{g}{2}|\tilde{\chi}_R|^2 \end{pmatrix}$$

$$h_{UP} = \begin{pmatrix} \frac{\delta}{2} + \frac{g}{4}|\tilde{\chi}_L|^2 + \frac{g}{2}|\tilde{\psi}_L|^2 & -1 \\ -1 & -\frac{\delta}{2} + \frac{g}{4}|\tilde{\chi}_R|^2 + \frac{g}{2}|\tilde{\psi}_R|^2 \end{pmatrix}$$

$$v = e^{-i\Delta\tau} \begin{pmatrix} \frac{g}{2}n_L & -1 \\ -1 & \frac{g}{2}n_R \end{pmatrix} + e^{-i2\Delta\tau} \begin{pmatrix} \frac{g}{4}\tilde{\psi}_L^*\tilde{\chi}_L & 0 \\ 0 & \frac{g}{4}\tilde{\psi}_R^*\tilde{\chi}_R \end{pmatrix},$$

where $n_{L(R)}$ is the total particle number on the left (right) side.

In an EP system, the LP-UP energy difference μ_{UL} , which is the Rabi-splitting determined by strong photon-exciton hybridization, is several orders of magnitude larger than the left-right energy difference μ_{LR} . In Eq. (4), for $\Delta \gg \delta, g$, the inter-branch block v carries a fast oscillating phase. Under the random phase approximation, we neglect this inter-branch coupling and obtain a pair of two-component equations for upper and lower EP condensates,

$$i\partial_\tau \begin{pmatrix} \tilde{\psi}_L \\ \tilde{\psi}_R \end{pmatrix} = h_L \begin{pmatrix} \tilde{\psi}_L \\ \tilde{\psi}_R \end{pmatrix}, \quad i\partial_\tau \begin{pmatrix} \tilde{\chi}_L \\ \tilde{\chi}_R \end{pmatrix} = h_U \begin{pmatrix} \tilde{\chi}_L \\ \tilde{\chi}_R \end{pmatrix}. \quad (5)$$

We note that the polariton-exchange process between LP and UP branches is effectively absent, and the particle numbers of UP and LP branches are approximately conserved in the time scale large than Rabi period. However, the existence of the upper polariton serves as a dynamical chemical potential to the lower polariton condensate, causing the density $n_{L/U}$ in lower/upper polariton only oscillate at a small amplitude around its

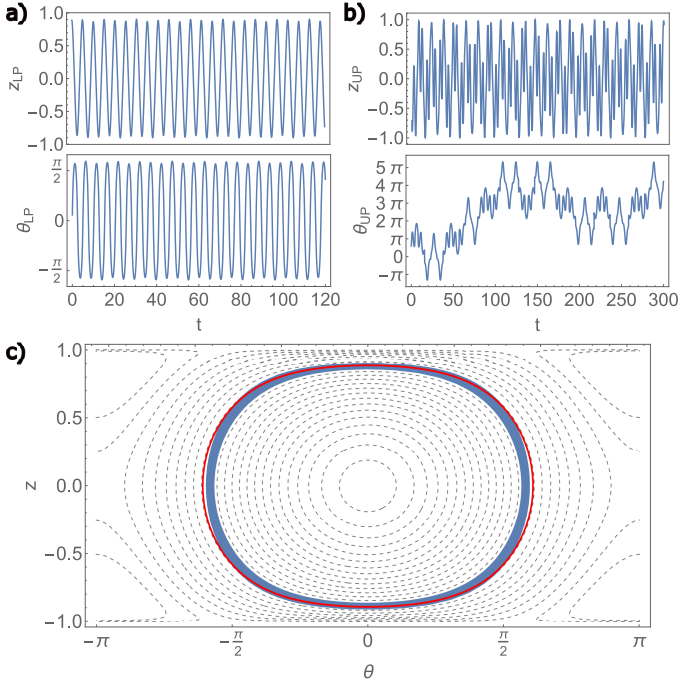


FIG. 3. Dynamics of LP and UP condensates for low UP filling. We take $n_{LP} = 0.95$ and $n_{UP} = 0.05$. (a) and (b) Time evolution of LP and UP condensates, respectively. (c) Phase-space trajectory of LP condensates corresponding to (a). The red trace is a closed trajectory for stabilized state of two-component LP-only model.

mean value. For the LP condensates, we parametrize $\psi_{L(R)} = \sqrt{n_{LP}(1 \pm z_{LP})}/2e^{i\theta_{LP,L(R)}}$ where n_{LP} is the total number of lower polaritons and $|z_{LP}| \leq 1$; Similar parametrization applies to the UP condensates. We transform Eq. (5) to

$$\begin{aligned}\dot{\theta}_\sigma &= \Lambda_\sigma(z_\sigma - z_{b,\sigma}) + \frac{z_\sigma}{\sqrt{1-z_\sigma^2}} \cos \theta_\sigma, \\ \dot{z}_\sigma &= -\sqrt{1-z_\sigma^2} \sin \theta_\sigma,\end{aligned}\quad (6)$$

where $\sigma \in \{LP, UP\}$, $\theta_\sigma = \theta_{\sigma,L} - \theta_{\sigma,R}$, and the dynamical chemical potential bias $z_{b,\sigma} = z_{0,\sigma} + c_\sigma z_{\bar{\sigma}}$ consists of two parts: $z_{0,\sigma} = -\frac{\delta}{2\Lambda_\sigma}$ with $\Lambda_{L/U} = gn_{L/U}/4$ and $c_\sigma = n_{\bar{\sigma}}/n_\sigma$. The chemical potential in one branch is dynamically influenced by its counterpart.

When the UP branches are insufficiently populated $n_L \gg n_U$, as shown in Fig. 3, we find that the LP condensates exhibit high-frequency but small-amplitude oscillations that are induced by the UP condensates. However, the UP condensates exhibit small-amplitude but chaotic oscillations due to the periodic driving force generated by the LP condensates through interactions. We justify that the two-component GP equation (3) is valid only for LP condensates in this limit.

In contrast, when the population of the two EP condensates are comparable, the temporal oscillations in one component can act as a dynamical driving force in the

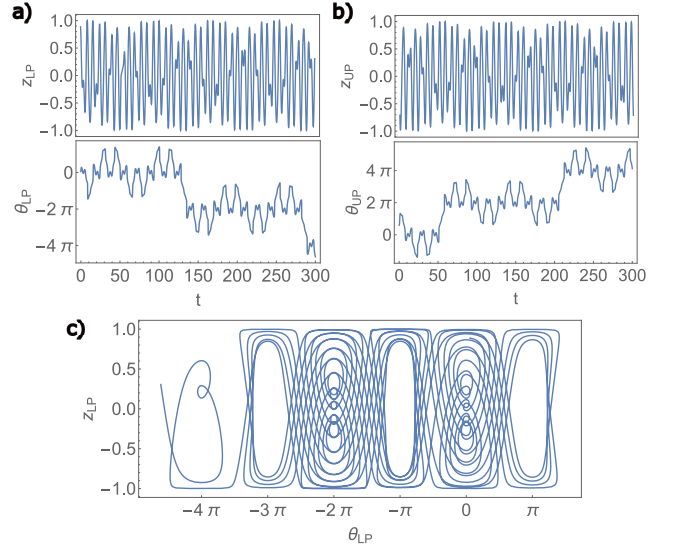


FIG. 4. Dynamics of LP and UP condensates for equal UP and LP fillings $n_{LP} = n_{UP} = 0.5$. (a) and (b) Time evolution of LP and UP condensates, respectively. (c) Phase-space trajectory of LP condensates corresponding to (a).

other. We always obtain chaotic behavior for both LP and UP condensates, as shown in Fig. 4.

Discussion. In this letter we have explored the wealth of possible behavior when nanofabricated electrical elements are incorporated into optical cavities, which provide additional and simultaneous probes of the condensates. However, the description of Eq. (1) assumes the existence of a well-defined and conserved condensates, as well as ignoring the presence of the thermally distributed EP states. The theory for a single non-equilibrium condensate coupled to a dynamical finite particle number reservoir is present in [12, 29], where the GP equation is used for the condensate which can adiabatically adjust to the minimal energy states near the single-polariton ground state. The processes of condensate re-population given by the non-condensate EP reservoir and condensate decay due to photon leaking are described by imaginary source and sink terms. The validation of our EP junction models depends on time scales. If the re-population and decay rates are slow compared to the Josephson frequency, then the GP equation (1) is valid and all the dynamical behaviors predicted in our work should be observed. However, if the decay time is too short, the oscillations may be damped due to the instability of the condensate. If the re-population processes are too fast, the oscillations will be replaced by a steady and phase-dependent flow of polaritons across the junction. In most cases, the actual chemical potential bias of the junction depends on the dynamical finite number reservoir, which is highly unpredictable in a non-equilibrium polariton gas. However, recent experiments [30, 31] measure non-condensate EP approaching the Bose-Einstein distribution as evidence of thermal equilibrium, showing that it is possible in this condition to achieve a steady state ideal

for the operation of this device.

We have also neglected the incoherent tunneling of the thermal population of polaritons due to finite temperature. This incoherent tunneling gives rise to a dissipated current in addition to the supercurrent of EP condensates, in analogy to the quasi-particle tunneling in superconducting Josephson junctions. We develop the corresponding “resistively shunted junction model” in a future work.

The pseudo spin of EP, closely connected to optical polarization, is not discussed here. We expect that in the quantum well the spin relaxation [32] could couple the EP condensates to dark exciton states. This mechanism should introduce even richer dynamics and provide a potential technique for detecting dark excitons.

The use of nanofabricated electrical elements provides not only a way to drive the condensates, but also a way

to measure the condensate density, since the capacitance of each side of the device will change with the dielectric density. Small variations in capacitance can be measured very precisely by their effect on the resonance frequency of co-fabricated circuits. The shift in capacitance can provide information on the total condensate density, including the possibility of observing “dark” condensates that are not optically observable. Nanofabrication has enabled the creation of single electron devices, the monitoring of single spins, and the control of superconducting qubits. We believe that its incorporation into optical cavities will lead to better understanding of EP condensates.

We thank B. Uchoa, A. Auerbach, and Y. Zhang for stimulating discussions. The work of H.-Y.X. is supported by the Dodge Family Fellowship granted by the University of Oklahoma.

-
- [1] M. H. Anderson, J. R. Ensher, M. R. Matthews, C. E. Wieman, and E. A. Cornell, Observation of bose-einstein condensation in a dilute atomic vapor, *Science* **269**, 198 (1995).
- [2] K. B. Davis, M. O. Mewes, M. R. Andrews, N. J. van Druten, D. S. Durfee, D. M. Kurn, and W. Ketterle, Bose-einstein condensation in a gas of sodium atoms, *Phys. Rev. Lett.* **75**, 3969 (1995).
- [3] B. Keimer, S. A. Kivelson, M. R. Norman, S. Uchida, and J. Zaanen, From quantum matter to high-temperature superconductivity in copper oxides, *Nature* **518**, 179 (2015).
- [4] Q. Cao, F. Grote, M. Hußmann, and S. Eigler, Emerging field of few-layered intercalated 2d materials, *Nanoscale Adv.* **3**, 963–982 (2021).
- [5] M. A. Nielsen and I. L. Chuang, *Quantum Computation and Quantum Information*, 2nd ed. (Cambridge University Press, 2010).
- [6] F. Arute *et al.*, Quantum supremacy using a programmable superconducting processor, *Nature* **574**, 505–510 (2019).
- [7] H. J. Kimble, The quantum internet, *Nature* **453**, 1023–1030 (2008).
- [8] C. L. Degen, F. Reinhard, and P. Cappellaro, Quantum sensing, *Rev. Mod. Phys.* **89**, 035002 (2017).
- [9] C. Gross and I. Bloch, Quantum simulations with ultracold atoms in optical lattices, *Science* **357**, 995 (2017).
- [10] J. Kasprzak, M. Richard, S. Kundermann, A. Baas, P. Jeambrun, J. M. J. Keeling, F. M. Marchetti, M. H. Szymańska, R. André, J. L. Staehli, V. Savona, P. B. Littlewood, B. Deveaud, and L. S. Dang, Bose–Einstein condensation of exciton polaritons, *Nature* **443**, 409 (2006).
- [11] H. Deng, H. Haug, and Y. Yamamoto, Exciton-polariton bose-einstein condensation, *Rev. Mod. Phys.* **82**, 1489 (2010).
- [12] I. Carusotto and C. Ciuti, Quantum fluids of light, *Rev. Mod. Phys.* **85**, 299 (2013).
- [13] H. Haug and S. W. Koch, *Quantum Theory of the Optical and Electronic Properties of Semiconductors*, 5th ed. (World Scientific Publishing Company, 2020).
- [14] C. Schneider, K. Winkler, M. D. Fraser, M. Kamp, Y. Yamamoto, E. A. Ostrovskaya, and S. Höfling, Exciton-polariton trapping and potential landscape engineering, *Reports on Progress in Physics* **80**, 016503 (2016).
- [15] C. W. Lai, N. Y. Kim, S. Utsunomiya, G. Roumpos, H. Deng, M. D. Fraser, T. Byrnes, P. Recher, N. Kumada, T. Fujisawa, and Y. Yamamoto, Coherent zero-state and π -state in an exciton–polariton condensate array, *Nature* **450**, 529 (2007).
- [16] E. A. Cerda-Méndez, D. N. Krizhanovskii, M. Wouters, R. Bradley, K. Biermann, K. Guda, R. Hey, P. V. Santos, D. Sarkar, and M. S. Skolnick, Polariton condensation in dynamic acoustic lattices, *Phys. Rev. Lett.* **105**, 116402 (2010).
- [17] T. Jacqmin, I. Carusotto, I. Sagnes, M. Abbarchi, D. D. Solnyshkov, G. Malpuech, E. Galopin, A. Lemaître, J. Bloch, and A. Amo, Direct observation of dirac cones and a flatband in a honeycomb lattice for polaritons, *Phys. Rev. Lett.* **112**, 116402 (2014).
- [18] C. E. Whittaker, E. Cancellieri, P. M. Walker, D. R. Gulevich, H. Schomerus, D. Vaitiekus, B. Royall, D. M. Whittaker, E. Clarke, I. V. Iorsh, I. A. Shelykh, M. S. Skolnick, and D. N. Krizhanovskii, Exciton polaritons in a two-dimensional lieb lattice with spin-orbit coupling, *Phys. Rev. Lett.* **120**, 097401 (2018).
- [19] S. Klemmt, T. H. Harder, O. A. Egorov, K. Winkler, R. Ge, M. A. Bandres, M. Emmerling, L. Worschech, T. C. H. Liew, M. Segev, C. Schneider, and S. Höfling, Exciton-polariton topological insulator, *Nature* **562**, 552 (2018).
- [20] R. Su, S. Ghosh, J. Wang, S. Liu, C. Diederichs, T. C. H. Liew, and Q. Xiong, Observation of exciton polariton condensation in a perovskite lattice at room temperature, *Nature Physics* **16**, 301 (2020).
- [21] C. W. Lai, G. Roumpos, A. Forchel, and Y. Yamamoto, First and second order coherence of exciton-polariton condensates, in *2008 Conference on Lasers and Electro-Optics and 2008 Conference on Quantum Electronics and Laser Science* (2008) pp. 1–2.
- [22] T. Horikiri, P. Schwendemann, A. Quattropani, S. Höfling, A. Forchel, and Y. Yamamoto, Higher order coherence of exciton-polariton condensates,

- Phys. Rev. B **81**, 033307 (2010).
- [23] X. L. Yang, S. H. Guo, F. T. Chan, K. W. Wong, and W. Y. Ching, Analytic solution of a two-dimensional hydrogen atom. i. nonrelativistic theory, Phys. Rev. A **43**, 1186 (1991).
- [24] S. L. Chuang, *Physics of Photonic Devices*, 2nd ed. (Wiley, 2009) p. 840.
- [25] S. I. Tsintzos, A. Tzimis, G. Stavrinidis, A. Trifonov, Z. Hatzopoulos, J. J. Baumberg, H. Ohadi, and P. G. Savvidis, Electrical tuning of nonlinearities in exciton-polariton condensates, Phys. Rev. Lett. **121**, 037401 (2018).
- [26] R. I. Kaitouni, O. El Daïf, A. Baas, M. Richard, T. Paraiso, P. Lugan, T. Guillet, F. Morier-Genoud, J. D. Ganière, J. L. Staehli, V. Savona, and B. Deveaud, Engineering the spatial confinement of exciton polaritons in semiconductors, Phys. Rev. B **74**, 155311 (2006).
- [27] Y. Sun, Y. Yoon, M. Steger, G. Liu, L. N. Pfeiffer, K. West, D. W. Snoke, and K. A. Nelson, Direct measurement of polariton-polariton interaction strength, Nature Physics **13**, 870 (2017).
- [28] S. Raghavan, A. Smerzi, S. Fantoni, and S. R. Shenoy, Coherent oscillations between two weakly coupled bose-einstein condensates: Josephson effects, π oscillations, and macroscopic quantum self-trapping, Phys. Rev. A **59**, 620 (1999).
- [29] M. Wouters and I. Carusotto, Excitations in a nonequilibrium bose-einstein condensate of exciton polaritons, Phys. Rev. Lett. **99**, 140402 (2007).
- [30] Y. Sun, P. Wen, Y. Yoon, G. Liu, M. Steger, L. N. Pfeiffer, K. West, D. W. Snoke, and K. A. Nelson, Bose-einstein condensation of long-lifetime polaritons in thermal equilibrium, Phys. Rev. Lett. **118**, 016602 (2017).
- [31] H. Alnatah, Q. Yao, J. Beaumariage, S. Mukherjee, M. C. Tam, Z. Wasilewski, K. West, K. Baldwin, L. N. Pfeiffer, and D. W. Snoke, Coherence measurements of polaritons in thermal equilibrium reveal a new power law for two-dimensional condensates (2023), arXiv:2308.05100 [cond-mat.quant-gas].
- [32] M. Z. Maialle, E. A. de Andrada e Silva, and L. J. Sham, Exciton spin dynamics in quantum wells, Phys. Rev. B **47**, 15776 (1993).
- [33] M. H. Szymańska, J. Keeling, and P. B. Littlewood, Nonequilibrium quantum condensation in an incoherently pumped dissipative system, Phys. Rev. Lett. **96**, 230602 (2006).
- [34] M. I. Vasilevskiy, D. G. Santiago-Pérez, C. Trallero-Giner, N. M. R. Peres, and A. Kavokin, Exciton polaritons in two-dimensional dichalcogenide layers placed in a planar microcavity: Tunable interaction between two bose-einstein condensates, Phys. Rev. B **92**, 245435 (2015).
- [35] Y. Huang, Q.-S. Tan, L.-B. Fu, and X. Wang, Coherence dynamics of a two-mode bose-einstein condensate coupled with the environment, Phys. Rev. A **88**, 063642 (2013).
- [36] M. Wouters and V. Savona, Stochastic classical field model for polariton condensates, Phys. Rev. B **79**, 165302 (2009).
- [37] F. Tassone and Y. Yamamoto, Exciton-exciton scattering dynamics in a semiconductor microcavity and stimulated scattering into polaritons, Phys. Rev. B **59**, 10830 (1999).
- [38] C. Ciuti, V. Savona, C. Piermarocchi, A. Quattropani, and P. Schwendimann, Role of the exchange of carriers in elastic exciton-exciton scattering in quantum wells, Phys. Rev. B **58**, 7926 (1998).
- [39] J. J. Hopfield, Theory of the Contribution of Excitons to the Complex Dielectric Constant of Crystals, Physical Review **112**, 1555 (1958).
- [40] R. Su, S. Ghosh, J. Wang, S. Liu, C. Diederichs, T. C. H. Liew, and Q. Xiong, Observation of exciton polariton condensation in a perovskite lattice at room temperature, Nature Physics **16**, 301 (2020).
- [41] A. Smerzi, S. Fantoni, S. Giovanazzi, and S. R. Shenoy, Quantum coherent atomic tunneling between two trapped bose-einstein condensates, Phys. Rev. Lett. **79**, 4950 (1997).
- [42] S. Giovanazzi, A. Smerzi, and S. Fantoni, Josephson effects in dilute bose-einstein condensates, Phys. Rev. Lett. **84**, 4521 (2000).

SUPPLEMENTAL MATERIAL:
Electrical Control of Exciton-Polariton Condensate Josephson Junctions

Hua Wang,^{1,*} Hong-Yi Xie,^{1,†} and Kieran Mullen¹

¹*Homer L. Dodge Department of Physics and Astronomy, Center for Quantum Research and Technology,
The University of Oklahoma, Norman, Oklahoma 73069, USA*

S1. JOSEPHSON TUNNELING ENERGY

We consider exciton Hamiltonian in a EP junction

$$H_0 = \sum_{\mathbf{K}} \left(E_{\nu\mathbf{K}} \hat{b}_{L,\nu\mathbf{K}}^\dagger \hat{b}_{L,\nu\mathbf{K}} + E_{\nu'\mathbf{K}} \hat{b}_{R,\nu'\mathbf{K}}^\dagger \hat{b}_{R,\nu'\mathbf{K}} \right), \quad (\text{S1})$$

where ν (ν') labels the exciton orbit on the left (right) side, $E_{\nu\mathbf{K}}$ is the exciton-band dispersion, and exciton creation operator reads[?]]

$$\hat{b}_{\kappa,\nu\mathbf{K}}^\dagger = \sum_{\mathbf{k}} \Phi_\nu(\mathbf{k}, \mathbf{K}) \hat{e}_{\kappa,\mathbf{k}}^\dagger \hat{h}_{\kappa,\mathbf{K}-\mathbf{k}}^\dagger, \quad (\text{S2})$$

with $\kappa \in \{L, R\}$, $\hat{e}_{\kappa,\mathbf{k}}^\dagger$ ($\hat{h}_{\kappa,\mathbf{k}}^\dagger$) being the creation operator of electron (hole) at momentum \mathbf{k} , \mathbf{K} the exciton COM momentum, and $\Phi_\nu(\mathbf{k}, \mathbf{K})$ the Fourier component of the ν -orbit wavefunction of excitons.

We derive the exciton tunneling energy from the single-particle tunneling Hamiltonian

$$H_T = \sum_{\mathbf{k}} \left(t_e \hat{e}_{R,\mathbf{k}}^\dagger \hat{e}_{L,\mathbf{k}} + t_h \hat{h}_{R,\mathbf{k}}^\dagger \hat{h}_{L,\mathbf{k}} + h.c. \right), \quad (\text{S3})$$

where the tunneling energies $t_{e,h}$ are material and device-geometry dependent. Defining the single-exciton states $|\Phi_{\kappa,\nu\mathbf{K}}\rangle \equiv \hat{b}_{\kappa,\nu\mathbf{K}}^\dagger |0\rangle$, where $|0\rangle$ is the physical vacuum of excitons, up to second order in $t_{e,h}$, we obtain the exciton left-to-right tunneling energy

$$J_{\nu'\nu}(\mathbf{K}) = \frac{1}{2} \sum_{\gamma} \langle \Phi_{R,\nu'\mathbf{K}} | H_T | \gamma \rangle \langle \gamma | H_T | \Phi_{L,\nu\mathbf{K}} \rangle \left(\frac{1}{E_{\nu\mathbf{K}} - \epsilon_\gamma} + \frac{1}{E_{\nu'\mathbf{K}} - \epsilon_\gamma} \right), \quad (\text{S4})$$

where the intermediate states $|\gamma\rangle \equiv \hat{e}_{\kappa,\mathbf{k}}^\dagger \hat{h}_{\kappa',\mathbf{K}-\mathbf{k}}^\dagger |0\rangle$ form a set of complete basis in electron-hole space. Finally, we can write done the exciton tunneling energy in Eq. (S4) in a simple form

$$J_{\nu'\nu}(\mathbf{K}) = t_e t_h \sum_{\mathbf{k}} \Phi_{\nu'}^*(\mathbf{k}, \mathbf{K}) \Phi_\nu(\mathbf{k}, \mathbf{K}) \left(\frac{1}{E_{\nu\mathbf{K}} - \epsilon_{\mathbf{k},\mathbf{K}-\mathbf{k}}} + \frac{1}{E_{\nu'\mathbf{K}} - \epsilon_{\mathbf{k},\mathbf{K}-\mathbf{k}}} \right), \quad (\text{S5})$$

where $\epsilon_{\mathbf{k},\mathbf{k}'} = \frac{\hbar^2 k^2}{2m_e} + \frac{\hbar^2 k'^2}{2m_h}$ is the energy of a pair of noninteracting electron and hole. For $\nu = \nu'$ and $\mathbf{K} = 0$, we obtain

$$J_{\nu\nu}(0) = 2t_e t_h \int \frac{|\Phi_\nu(\mathbf{k}, 0)|^2}{E_\nu - \frac{\hbar^2 k^2}{2\mu}} d^2\mathbf{k}, \quad (\text{S6})$$

where $\mu \equiv m_e m_h / (m_e + m_h)$ is the reduced mass of an e-h pair. For two-dimensional excitons in 1s ($\nu = 0$) state

* hua.wang.phys@ou.edu

† hongyi.xie-1@ou.edu

$\Phi_0(k, 0) = \sqrt{2\pi}2a(1 + a^2|k|^2)^{-3/2}$, we evaluate the momentum integral and obtain tunneling energy

$$J = -\frac{16\pi^2}{3} \frac{t_\epsilon t_h}{|E_0|}. \quad (\text{S7})$$

where the binding energy $|E_0| = \hbar^2/(2\mu a^2)$, with a being the Bohr radius.

S2. GP EQUATIONS IN ROTATING FRAME

The four-component GP equations read $i\partial_t\Psi = H[\Psi^*, \Psi]\Psi$, where $\Psi = (\psi_L \ \psi_R \ \chi_L \ \chi_R)^T$ and the effective Hamiltonian takes the block form $H = \begin{pmatrix} H_L & V \\ V^\dagger & H_U \end{pmatrix}$, where

$$\begin{aligned} H_L &= \begin{pmatrix} \frac{\delta-\Delta}{2} + \frac{g}{4}|\psi_L|^2 + \frac{g}{2}|\chi_L|^2 & -1 \\ -1 & -\frac{\delta+\Delta}{2} + \frac{g}{4}|\psi_R|^2 + \frac{g}{2}|\chi_R|^2 \end{pmatrix}, & V &= \begin{pmatrix} \frac{g}{4}\psi_L^*\chi_L + \frac{g}{2}n_L & -1 \\ -1 & \frac{g}{4}\psi_R^*\chi_R + \frac{g}{2}n_R \end{pmatrix}, \\ H_U &= \begin{pmatrix} \frac{\delta+\Delta}{2} + \frac{g}{4}|\chi_L|^2 + \frac{g}{2}|\psi_L|^2 & -1 \\ -1 & -\frac{\delta-\Delta}{2} + \frac{g}{4}|\chi_R|^2 + \frac{g}{2}|\psi_R|^2 \end{pmatrix} \end{aligned} \quad (\text{S8})$$

with $n_\kappa = |\psi_\kappa|^2 + |\chi_\kappa|^2$ being the total density on $\kappa \in \{L, R\}$ side. For $\Delta \gg \delta, g$, we decompose the Hamiltonian into two parts $H = H_\Delta + H'$, where

$$H_\Delta = \text{diag}\{-\Delta/2, -\Delta/2, \Delta/2, \Delta/2\}. \quad (\text{S9})$$

Performing a ‘‘rotating frame’’ transformation, $(\tilde{\psi}_L \ \tilde{\psi}_R \ \tilde{\chi}_L \ \tilde{\chi}_R)^T \equiv e^{-iH_\Delta t}\Psi$ and $\begin{pmatrix} h_L & v \\ v^\dagger & h_U \end{pmatrix} \equiv e^{iH_\Delta t}H'e^{-iH_\Delta t}$, we transform the GP equations to Eq. (4).